Precipitates in As-Cast and Heat-Treated ASTM F75 Co-Cr-Mo-C Alloys Containing Si and/or Mn

ALFIRANO, SHINGO MINETA, SHIGENOBU NAMBA, TAKASHI YONEDA, KYOSUKE UEDA, and TAKAYUKI NARUSHIMA

The effect of the addition of Si or Mn to ASTM F75 Co-28Cr-6Mo-0.25C alloys on precipitate formation as well as dissolution during solution treatment was investigated. Three alloys—Co-28Cr-6Mo-0.25C-1Si (1Si), Co-28Cr-6Mo-0.25C-1Mn (1Mn), and Co-28Cr-6Mo-0.25C-1Si-1Mn (1Si1Mn)—were heat treated from 1448 K to 1548 K (1175 °C to 1275 °C) for a holding time of up to 43.2 ks. In the case of the as-cast 1Si and 1Si1Mn alloys, the precipitates were $M_{23}C_6$-type carbide, η phase (M_6C-$M_{12}C$–type carbide), and π phase (M_2T_3X-type carbide with a β-Mn structure), while in the case of the as-cast 1Mn alloy, $M_{23}C_6$-type carbide and η phase were detected. The 1Si and 1Si1Mn alloys required longer heat-treatment times for complete precipitate dissolution than did the 1Mn alloys. During the solution treatment, blocky dense $M_{23}C_6$-type carbide was observed in all the alloys over the temperature range of 1448 K to 1498 K (1175 °C to 1225 °C). At the heat-treatment temperature of 1523 K (1250 °C), starlike precipitates with stripe patterns—comprising $M_{23}C_6$-type carbide and metallic face-centered-cubic (fcc) γ phase—were detected in the 1Si and 1Si1Mn alloys. A π phase was observed in the 1Si and 1Si1Mn alloys heat treated at 1523 K and 1548 K (1250 °C and 1275 °C) and in the 1Mn alloy heat treated at 1548 K (1275 °C); its morphology was starlike-dense. The addition of Si appeared to promote the formation of the π phase in Co-28Cr-6Mo-0.25C alloys at 1523 K and 1548 K (1250 °C and 1275 °C). Thus, the addition of Si and Mn affects the phase and morphology of the carbide precipitates in biomedical Co-Cr-Mo alloys.

DOI: 10.1007/s11661-011-0604-4

I. INTRODUCTION

THE ASTM F75 cobalt-chromium-molybdenum (Co-Cr-Mo) alloys are used in the preparation of alloy castings by the investment casting technique.[1,2] These alloy castings are widely applied in surgical implants owing to their excellent corrosion and wear resistance and mechanical properties.[3–5] The alloy components prepared by investment casting exhibit a microstructure comprising a Co-rich dendrite matrix and interdendritic and grain boundary precipitates.[6–10] In the as-cast ASTM F75 Co-Cr-Mo alloys, the main precipitate was consistently identified as the $M_{23}C_6$-type carbide, wherein M refers to metallic elements such as Cr. Other phases such as the M_6C-$M_{12}C$–type carbide (η phase)[11–14] and intermetallic σ phase (Co(Cr,Mo)) were identified as minor precipitates. The possible precipitation of M_7C_3-type carbide in the ASTM F75 Co-Cr-Mo alloys during solidification was also suggested, but its presence was not confirmed.[9] As-cast Co-Cr-Mo alloys are typically subjected to heat treatment in order to eliminate casting defects and to improve their mechanical properties. The behavior of carbides in Co-Cr-Mo alloys during heat treatment was previously investigated by several research groups, including the present authors.[10,15–20]

It is known that the addition of alloying elements to biomedical Co-Cr-Mo alloys affects the phases of precipitates. For example, the tendency toward σ-phase formation increases with the Fe content in Co-Cr-Mo-(5 to 20 mass pct)Fe alloys.[21] The presence of blocky MC-type carbides comprising Zr and carbon has been demonstrated in Co-Cr-Mo alloys when 0.05 to 0.1 mass pct Zr and 0.22 to 0.23 mass pct C were added.[22] Moreover, note that nitrogen is known to suppress the formation of the σ phase.[4] In a prior study, the present authors investigated the effect of the addition of carbon on the phase and morphology of precipitates in as-cast and heat-treated ASTM F75 Co-28 mass pct Cr-6 mass pct Mo-(0.12 to 0.35)mass pct C alloys.[10] We detected a π phase (M_2T_3X-type carbide with a β-Mn structure;[23–26] M and T: metallic elements; X: carbon) in the as-cast alloy with 0.15 mass pct C and in the alloys with (0.15 to 0.35) mass pct C heat treated at 1548 K (1275 °C) for a short holding time of less than 1.8 ks.

In this study, Si and Mn were used as the alloying elements in biomedical Co-Cr-Mo-C alloys. The ASTM F75 standard permits the addition of Si and Mn up to 1

ALFIRANO and SHINGO MINETA, Graduate Students, KYOSUKE UEDA, Assistant Professor, and TAKAYUKI NARUSHIMA, Professor, are with the Department of Materials Processing, Graduate School of Engineering, Tohoku University, Sendai 980-8579, Japan. Contact e-mail: a8td9511@stu.material.tohoku.ac.jp SHIGENOBU NAMBA, Senior Research Metallurgist, is with the Materials Research Laboratory, Kobe Steel, Ltd., Kobe 651-2271, Japan. TAKASHI YONEDA, President, is with Yoneda Advanced Casting Co., Ltd., Takaoka 933-0951, Japan.

Manuscript submitted August 30, 2010.
Article published online February 2, 2011

mass pct.[1] We investigated the effect of the addition of 1 mass pct Si and/or 1 mass pct Mn to ASTM F75 Co-28 mass pct Cr-6 mass pct Mo-0.25 mass pct C alloy on the precipitates formed under as-cast conditions; further, the formation and dissolution of precipitates during solution treatment were also investigated. The precipitates formed in the as-cast and heat-treated alloys were electrolytically extracted, and their phase and morphology were precisely determined. Hereafter, for brevity, the chemical composition of the alloys is denoted by mass percent and the notation mass percent is omitted.

II. EXPERIMENTAL PROCEDURE

A. *Specimens*

The chemical compositions of the alloys used in this study are listed in Table I. The ASTM F75 Co-28Cr-6Mo-0.25C alloys with the addition of 1 mass pct Si, 1 mass pct Mn, and 1 mass pct Si + 1 mass pct Mn, and without addition are referred as 1Si, 1Mn, 1Si1Mn, and 0Si0Mn, respectively (Table I). In this study, the 1Si, 1Mn, and 1Si1Mn alloys were primarily used, and the results obtained using these alloys are compared with those obtained using the 0Si0Mn alloy. The phase and morphology of the precipitates in the 0Si0Mn alloy were reported in a previous study.[10] However, the 0Si0Mn alloy data shown in Figures 1 through 3 in Section III are the original data.

Alloy ingots—with a diameter of 34 mm and height of 100 mm—were prepared using an induction melting furnace under Ar atmosphere and cast in a copper mold. These ingots were cut into disk shapes of 34-mm diameter and 5-mm thickness, which were then cut into four equal parts.

B. *Heat Treatment*

Heat treatment was performed in an electric resistance tube furnace at 1448 K, 1473 K, 1498 K, 1523 K, and 1548 K (1175 °C, 1200 °C, 1225 °C, 1250 °C, and 1275 °C) for 0, 1.8, 7.2, 21.6, and 43.2 ks in an atmosphere of high-purity Ar gas supplied at a gas flow rate of 1.7×10^{-6} m^3 s^{-1}. The heat treatment was initiated by inserting the specimens into the tube furnace maintained at the specified temperature under flowing Ar gas. The specimen temperature reached the specified value 0.6 ks after being placed in the hot zone of the tube furnace. The specimens were water quenched immediately after the completion of the heat treatment. The holding time of 0 ks implies that the specimens were water quenched immediately after the temperature reached the specified values (1448 K to 1548 K (1175 °C to 1275 °C)).

C. *Analysis of Specimens*

The specimens were cut into the thickness direction, and the cross section was mechanically ground with emery paper (maximum grit size: 1500) and polished with 1-μm diamond paste. The specimens were electrolytically etched in a 10 pct H_2SO_4-methanol solution at 6 V for microstructural observations. The microstructures of the as-cast and heat-treated alloys were observed using an optical microscope (OM, Olympus, Tokyo, BX60M) and a scanning electron microscope (SEM, Philips, Hillsboro, OR, XL30FEG). An electron-probe microanalyzer (EPMA, JEOL, Tokyo, JXA-8200) and a field emission EPMA (FE EPMA, JEOL, JXA-8530F) were used for the compositional analyses of the microstructures and precipitates. Observations using thin foil transmission electron microscopy (TEM, JEOL, JEM-2100) were conducted for the precipitates in the heat-treated alloys. The precipitates formed in the as-cast and heat-treated alloys were electrolytically extracted at room temperature in a 10 pct H_2SO_4 aqueous solution at 2 V. The phases of the extracted precipitates were identified using X-ray diffraction (XRD, Bruker AXS, Karlsruhe, Germany, D8 Advance), and the XRD patterns were obtained using Cu K_α radiation. The morphologies of the extracted precipitates were observed using the SEM.

III. RESULTS

A. *Microstructures and Types of Precipitates in As-Cast Alloys*

The microstructures of the as-cast 1Si, 1Mn, 1SiMn, and 0Si0Mn alloys are shown in Figure 1. The microstructure observed in these alloys typically consisted of a dendrite matrix and interdendritic and grain boundary precipitates. The content and size of the precipitates in the as-cast alloys, which were calculated using the OM images of the microstructure, are shown in Figure 2.

The XRD patterns of the precipitates electrolytically extracted from the as-cast alloys are shown in Figure 3. The γ phase, shown in Figure 3, indicates a Co-based alloy with face-centered-cubic (fcc) structure, which is a matrix but not a precipitate. The precipitates detected in the as-cast alloys are summarized in Table II. The precipitates in the as-cast 1Si and 1Si1Mn alloys were $M_{23}C_6$-type carbide, η phase (M_6C-$M_{12}C$-type carbide), and π phase (M_2T_3X-type carbide with a β-Mn structure); $M_{23}C_6$-type carbide and η phase were observed in the as-cast 1Mn and 0Si0Mn alloys.

Table I. Chemical Compositions of the Alloys Used in This Study (Mass Percent)

Abbreviation	Cr	Mo	C	Si	Mn	P	S	Co
1Si	29.17	6.22	0.23	0.96	0.08	<0.001	<0.001	bal.
1Mn	27.86	6.03	0.25	0.11	0.97	<0.001	<0.001	bal.
1Si1Mn	27.96	6.09	0.26	0.98	1.02	<0.001	<0.001	bal.
0Si0Mn	27.70	6.11	0.26	0.09	0.039	<0.001	<0.001	bal.

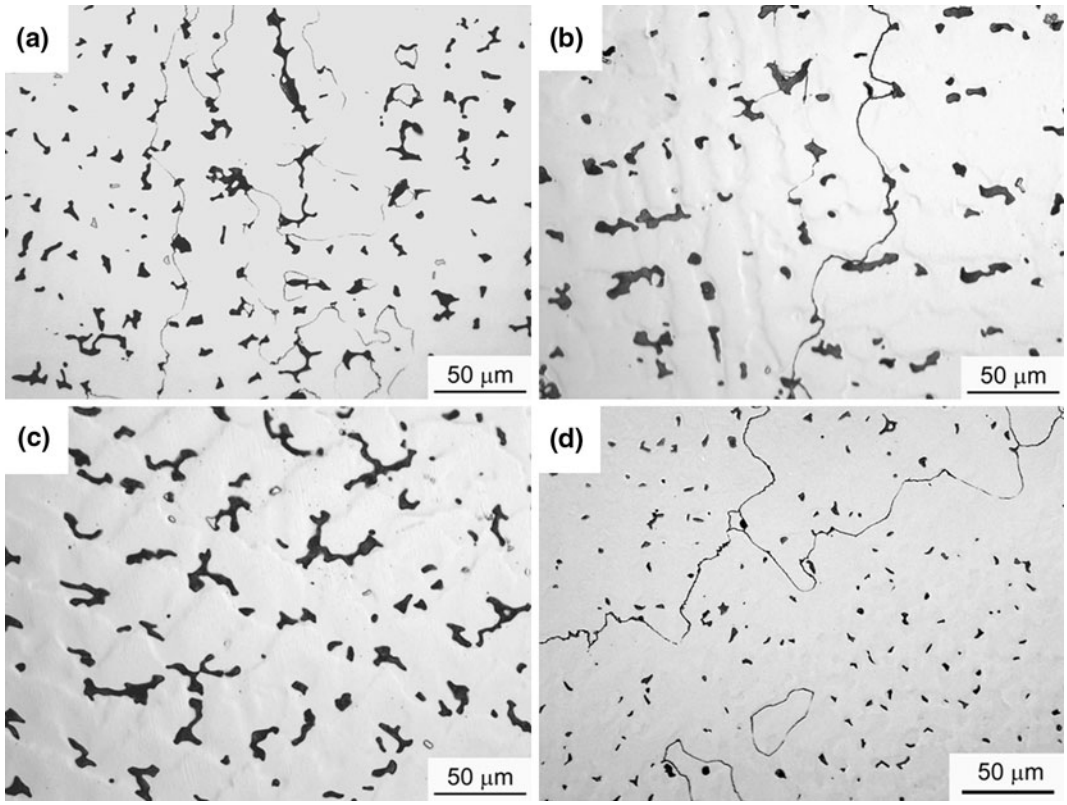

Fig. 1—Microstructure of the as-cast (*a*) 1Si, (*b*) 1Mn, (*c*) 1Si1Mn, and (*d*) 0Si0Mn alloys.

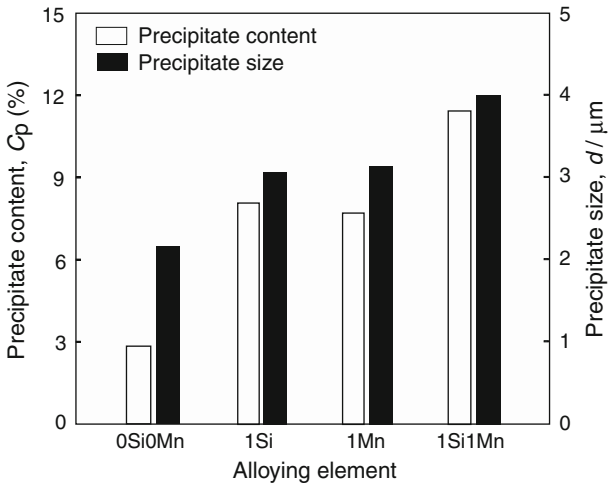

Fig. 2—Effect of the addition of Si and Mn on the content and size of precipitates in as-cast alloys.

B. *Microstructural Change in Alloys during Solution Treatment*

The microstructures of the 1Si, 1Mn, and 1Si1Mn alloys after heat treatment at various temperatures for a holding time of 1.8 ks are shown in Figure 4. The dissolution level of the precipitates depended on the heat-treatment temperature and alloy composition.

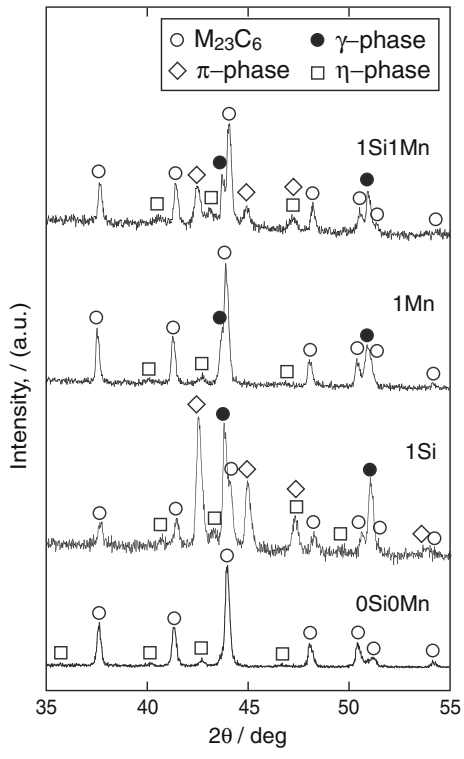

Fig. 3—XRD patterns of precipitates electrolytically extracted from as-cast 1Si, 1Mn, Si1Mn, and 0Si0Mn alloys.

In the alloys containing Si, complete precipitate dissolution was not observed after 1.8 ks even at the highest temperature used in this study, 1548 K (1275 °C) (Figures 4(c) and (i)). For complete precipitate dissolution, heat treatment was required at 1548 K (1275 °C) for 43.2 ks in the case of the 1Si alloy and at 1523 K (1250 °C) for 43.2 ks or 1548 K (1275 °C) for 21.6 ks in the case of the 1Si1Mn alloy. In contrast, the precipitates in the 1Mn alloy were completely dissolved after heat treatment at 1523 K and 1548 K (1250 °C and 1275 °C) for 1.8 ks, as shown in Figures 4(e) and (f), respectively. Based on the microstructural changes after heat treatment, complete precipitate dissolution conditions can be determined; these conditions are summarized in Figure 5.

Table II. Phase of Precipitates Observed in As-Cast Alloys

Alloy	$M_{23}C_6$ Type	η Phase	π Phase
1Si	Δ	Δ	◎
1Mn	◎	Δ	ND
1Si1Mn	◎	Δ	Δ
0Si0Mn	◎	Δ	ND

◎: main, Δ: minor, and ND: not detected.

C. *Types and Morphologies of Precipitates in Heat-Treated Alloys*

The precipitates observed under the incomplete precipitate dissolution conditions were electrolytically extracted from the alloys and then identified by XRD. Figure 6 shows typical results in the XRD patterns of the precipitates, which were extracted from the alloys after heat treatment at various temperatures for a holding time of 1.8 ks. The precipitate phases detected in the alloys under as-cast conditions and after heat treatment are summarized in Figure 7. In this figure, the description at each experimental point illustrates the order of intensity of the strongest peak in the XRD pattern for each precipitate; for example, "θ + π" (1Si alloy heat-treated at 1523 K (1250 °C) for 0 ks) implies that the strongest peak intensity of θ ($M_{23}C_6$-type carbide) is greater than that of the π phase. The main precipitates observed after heat treatment at higher temperatures such as 1548 K (1275 °C) were π phase, whereas the $M_{23}C_6$-type carbide was primarily observed in all the alloys heat treated from 1448 K to 1498 K (1175 °C to 1225 °C).

An unknown phase was detected in the region near the complete-incomplete dissolution boundary of the 1Si alloy at 1548 K (1275 °C) and the 1Si1Mn alloy at 1523 K and 1548 K (1250 °C and 1275 °C). The phase

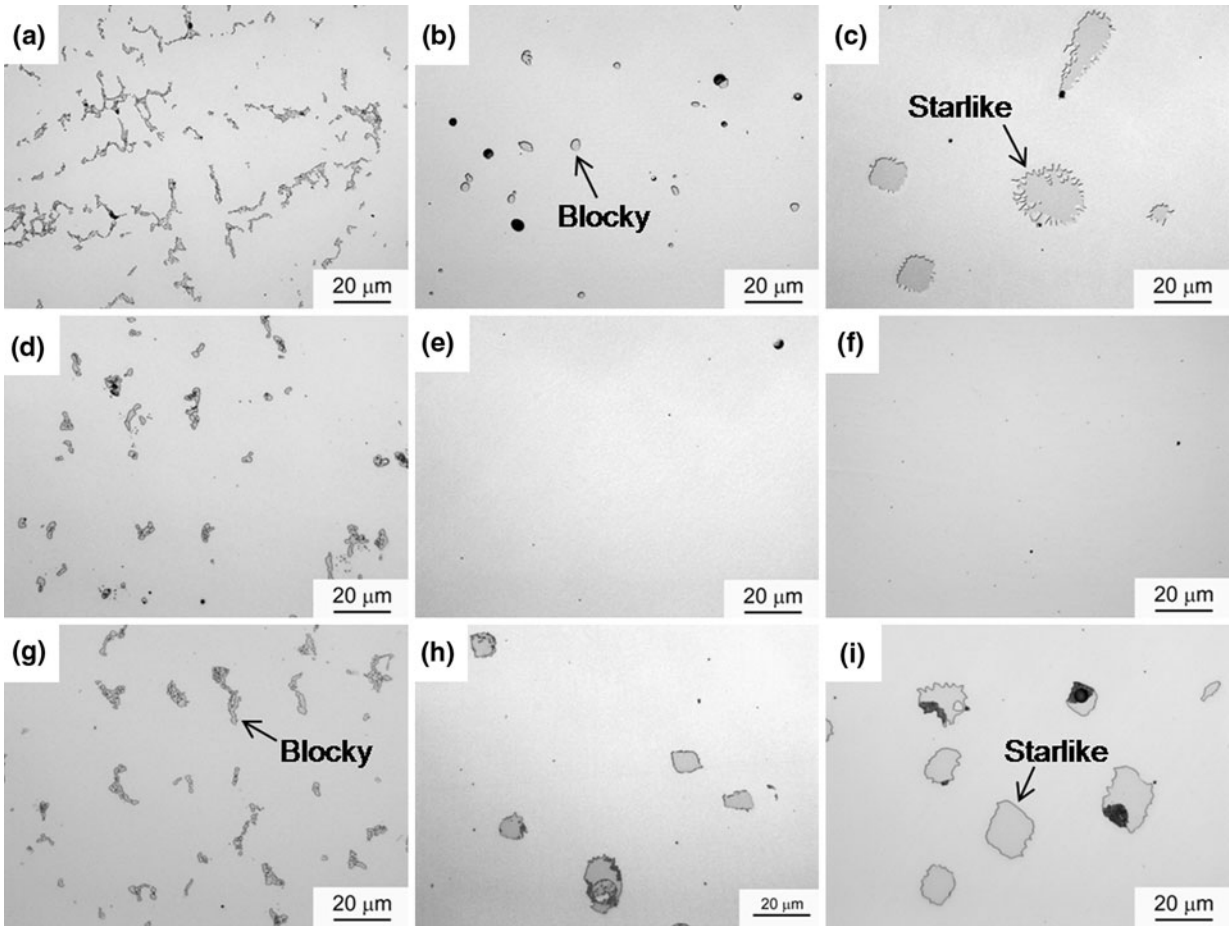

Fig. 4—Microstructure of (*a*) through (*c*) 1Si alloy, (*d*) through (*f*) 1Mn alloy, and (*g*) through (*i*) 1Si1Mn alloy after heat treatment at (a), (d), and (g) 1448 K (1175 °C), (b), (e), and (h) 1523 K (1250 °C), and (c), (f), and (i) 1548 K (1275 °C) for 1.8 ks.

and chemical composition of this phase were not clarified because the phase fraction was very small.

Two precipitate shapes—blocky and starlike—were observed, as shown in Figure 4. In all the alloys heat treated over the temperature range of 1448 K to 1498 K (1175 °C to 1225 °C), the morphology of the $M_{23}C_6$-type carbide was blocky-dense. Here, "dense" means that the appearance in the OM images after etching was uniform. A typical blocky-dense $M_{23}C_6$-type carbide electrolytically extracted from the 1Si alloy after heat treatment at 1523 K (1250 °C) for 21.6 ks is shown in Figure 8(a). At 1548 K (1275 °C), the precipitate shape formed in all the alloys was primarily starlike (Figure 8 (b)). The starlike precipitate had two types of appearances—dense and stripe patterned—as shown in Figures 9(a) and (b), respectively. TEM analysis revealed that the starlike-dense precipitate was π phase, as shown in Figures 10(a) through (c), and that the starlike precipitate with stripe patterns consisted of $M_{23}C_6$-type carbide and metallic fcc γ phase. The morphologies of the precipitates are summarized in Table III.

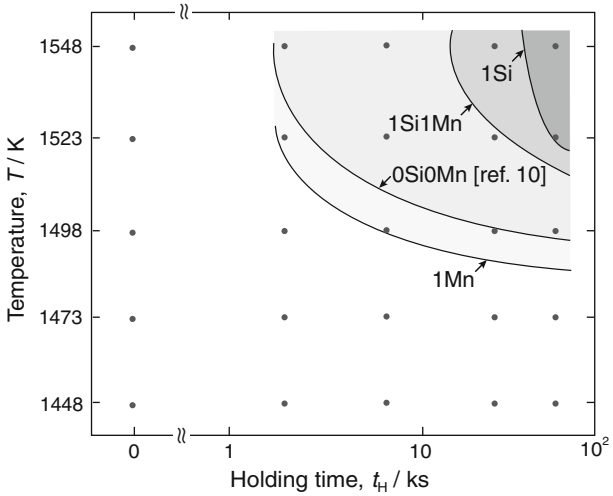

Fig. 5—Heat-treatment conditions for complete precipitate dissolution in Co-Cr-Mo-C-Si-Mn alloys.

IV. DISCUSSION

The precipitates observed in the alloys were $M_{23}C_6$-type carbide, η phase, and π phase, but M_7C_3-type carbide and intermetallic σ phase were not detected. The carbon content of the alloys used in this study was constant at 0.25 mass pct. It is known that the σ phase reacts with the solute carbon to form $M_{23}C_6$-type carbide and η phase during the solidification of Co-Cr-Mo-C alloys.[2] The carbon content of 0.25 mass pct was sufficient for progressing the reaction between σ phase and solute carbon, but it appeared to be insufficient for the formation of the M_7C_3-type carbide in ASTM F75 Co-Cr-Mo-C-Si-Mn alloys.

A π phase was observed in 1Si and 1Si1Mn alloys under the as-cast condition and after heat treatment at 1523 K and 1548 K (1250 °C and 1275 °C). On the other hand, in the 1Mn alloy, the π phase was detected only after heat treatment at 1548 K (1275 °C) for 0 ks as a minor precipitate similar to the case of the 0Si0Mn alloy.[10] Table IV demonstrates the chemical compositions of $M_{23}C_6$-type carbide and π phase, which were measured using FE EPMA. It was found that Si was slightly enriched in the π phase and was poor in the $M_{23}C_6$-type carbide. In the Co-Cr-Mo-C alloy system, as previously suggested by the present authors, the

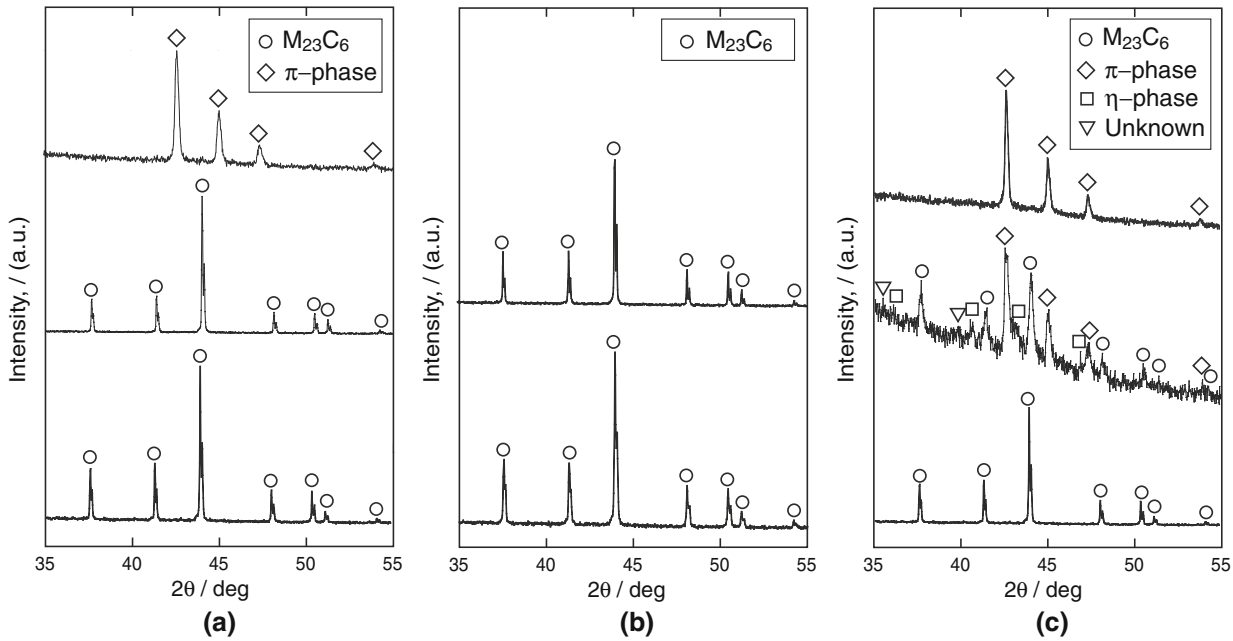

Fig. 6—XRD patterns of precipitates electrolytically extracted from heat-treated (*a*) 1Si, (*b*) 1Mn, and (*c*) 1Si1Mn alloys at various temperatures for 1.8 ks.

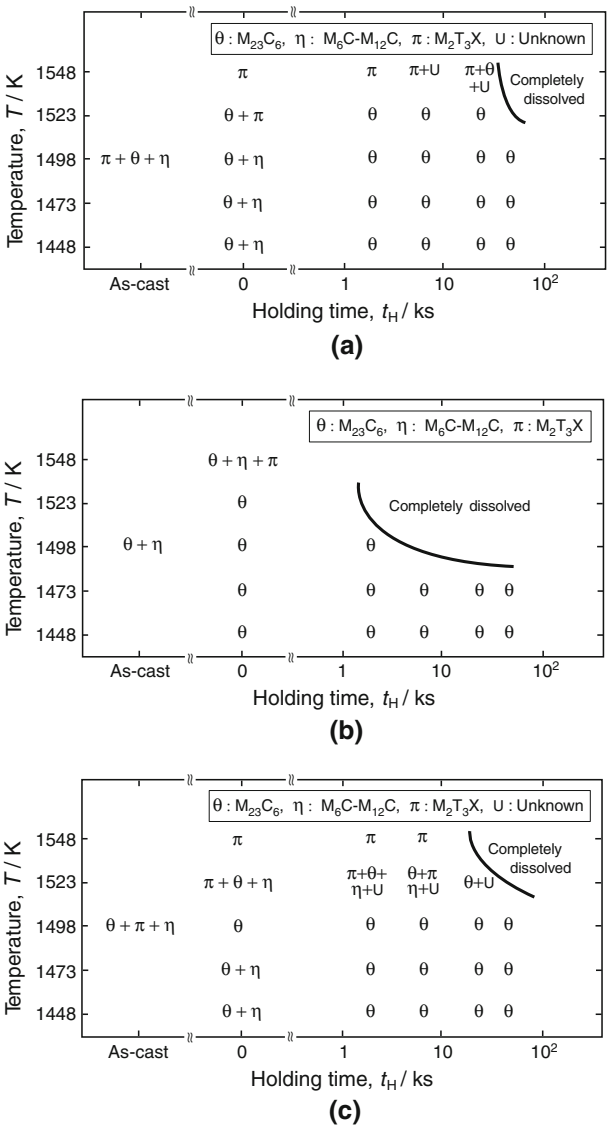

Fig. 7—Phases of precipitates in (*a*) 1Si, (*b*) 1Mn, and (*c*) 1Si1Mn alloys during solution treatment.

formation of the π phase during heat treatment is related to partial melting in the alloys.[10] The relative intensities of the strongest peaks in the XRD patterns for each precipitate in the alloys after heat treatment at various temperatures for 0 ks are shown in Figure 11; these relative intensities reflect the phase fraction of precipitates. The π phase was formed at higher temperatures, where partial melting was speculated to occur. These results suggest that the addition of Si and partial melting in alloys appears to promote π-phase formation. The EPMA analysis of the as-cast alloys showed that Cr, Mo, C, and Si were enriched in the interdendritic parts; the enrichment of Mn was also detected but less significantly. The interdendritic parts in the 1Si and 1Si1Mn alloys partially melt at lower temperatures than those in the 1Mn alloy. Therefore, the temperature at which the π phase was observed in the 1Si and 1Si1Mn alloys was 25 K (25 °C) lower than that at which the π phase was observed in the 1Mn alloy.

It is important to understand the complete precipitate dissolution conditions in Co-Cr-Mo alloys for ensuring effective heat treatment of alloy castings and thermomechanical treatment of wrought products. Several investigations on the dissolution of precipitates were conducted previously.[8–10,15–20] However, the effect of alloying elements on the dissolution behavior of precipitates was not reported for biomedical Co-Cr-Mo alloys. In this study, complete precipitate dissolution could be achieved in all the alloys by heat treatment. The Si addition increased the holding time for complete precipitate dissolution, while in the case of Mn addition, the precipitates dissolved in a short holding time. Since the content and size of the precipitates in the as-cast 1Si and 1Mn alloys were almost identical, as shown in Figure 2, the difference in the precipitate phases and microstructures in the as-cast and heat-treated alloys appeared to affect the apparent dissolution rates. The π phase was found in the as-cast 1Si and 1Si1Mn alloys but not in the as-cast 1Mn alloy. During the solution treatment, it is natural to expect the precipitates to be dissolved. On the other hand, the π phase appeared to be formed during the initial heat treatment at 1523 K and 1548 K (1250 °C

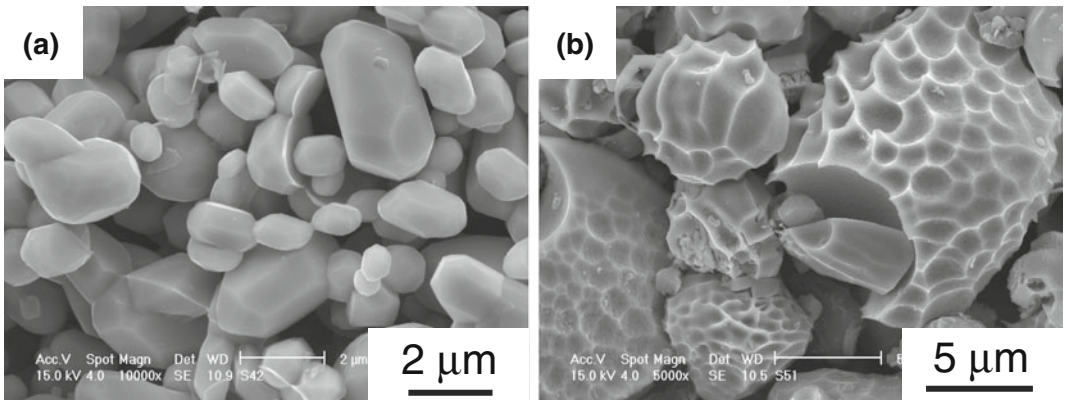

Fig. 8—SEM images of (*a*) blocky and (*b*) starlike precipitates electrolytically extracted from 1Si alloy heat treated at 1523 K (1250 °C) for 21.6 ks and 1548 K (1275 °C) for 1.8 ks, respectively.

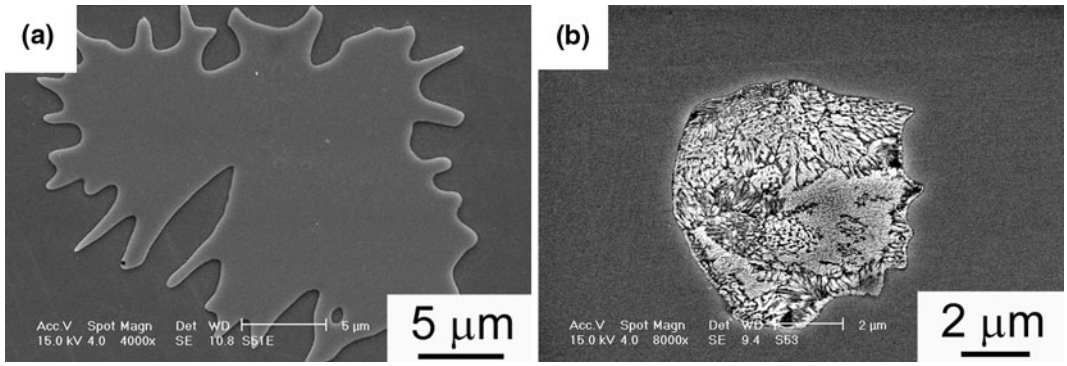

Fig. 9—SEM images of starlike (*a*) dense and (*b*) stripe-patterned precipitates in 1Si alloys heat treated at 1548 K (1275 °C) for 21.6 ks.

and 1275 °C) when coexisting with the melt; this causes an increase in the holding time for complete precipitate dissolution of 1Si and 1Si1Mn alloys at these temperatures. Moreover, it is known that the thermodynamic activity of carbon in iron-based alloys is increased by the addition of Si but is decreased by the addition of Mn.[27] Although data on carbon activity in Co-Cr-Mo alloys were reported previously, an increase in the carbon activity in 1Si and 1Si1Mn alloys is another possible mechanism that decreases the dissolution rates and increases the holding time for complete precipitate dissolution. The decrease of carbon activity in the 1Mn alloy could increase the apparent dissolution rate of precipitates, resulting in a short holding time for complete precipitate dissolution (Figure 5).

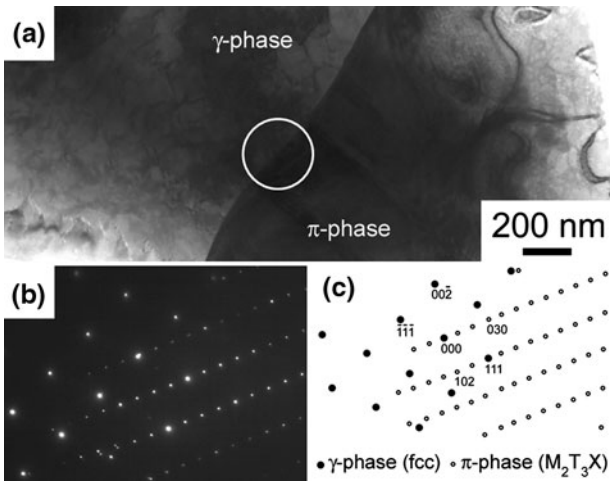

Fig. 10—TEM analysis of starlike-dense precipitate in 1Si1Mn alloy heat treated at 1548 K (1275 °C) for 1.8 ks: (*a*) bright-field image, (*b*) associated diffraction pattern, and (*c*) schematic diagram identifying reflections in (b). Beam directions are along [110] of γ phase and [201] of π phase.

Starlike precipitates were observed after heat treatment at 1523 K and 1548 K (1250 °C and 1275 °C) in the alloys, particularly in the 1Si and 1Si1Mn alloys. The presence of starlike precipitates in biomedical Co-Cr-Mo alloys was previously reported in the literature.[8–10] Clemow and Daniell observed starlike carbides in Co-28.75Cr-5.3Mo-0.28C-0.78Mn-0.88Si-0.60Fe-2Ni-0.43W alloy after heat treatment at 1503 K, 1523 K, and 1543 K (1230 °C, 1250 °C, and 1270 °C).[8] They stated that this distinctive starlike shape could be attributed to incipient melting around the edges of the M_6C-type carbides. The formation mechanism of starlike precipitates in this study is probably related to partial melting at the interface of the precipitate and matrix, as suggested by Clemow and Daniell. Both the π-phase formation and starlike morphology appear to be closely related to the partial melting in the alloys, which was caused by nonuniformities in the as-cast alloys.

Table III. Morphologies of the Precipitates in the Heat-Treated Alloys

Temperature, T [K (°C)]	Phase	Alloy	Morphology (Holding Time)
1448–1498 (1175–1225)	$M_{23}C_6$	1Si	blocky-dense
		1Mn	
		1Si1Mn	
1523 (1250)	$M_{23}C_6$	1Si	starlike-stripe (0 ks)
			blocky-dense (1.8 ~ 21.6 ks)
		1Mn	blocky-dense
		1Si1Mn	starlike-stripe
	π phase	1Si	starlike-dense
		1Si1Mn	
1548 (1275)	$M_{23}C_6$	1Si	starlike-stripe
		1Mn	starlike-stripe or blocky-dense
	π phase	1Si	starlike-dense
		1Mn	
		1Si1Mn	

Table IV. Chemical Compositions of $M_{23}C_6$-Type Carbide and π Phase (Mass Percent)

Phase	Alloys	Co	Cr	Mo	C	Si	Mn
$M_{23}C_6$ type	1Si (1448 K (1175 °C), 1.8 ks)	16.9	65.1	12.4	5.5	0.1	ND
	1Mn (1448 K (1175 °C), 1.8 ks)	17.7	63.8	12.3	5.6	ND	0.6
	1Si1Mn (1448 K (1175 °C), 1.8 ks)	15.9	65.3	12.3	5.7	0.1	0.7
π phase	1Si (1548 K (1275 °C), 1.8 ks)	40.6	37.9	18.0	2.2	1.3	ND
	1Mn (1548 K (1275 °C), 0 ks)	39.6	39.4	17.9	2.3	ND	0.8
	1Si1Mn (1548 K (1275 °C), 1.8 ks)	36.6	38.8	19.8	2.7	1.2	0.9

ND: not detected.

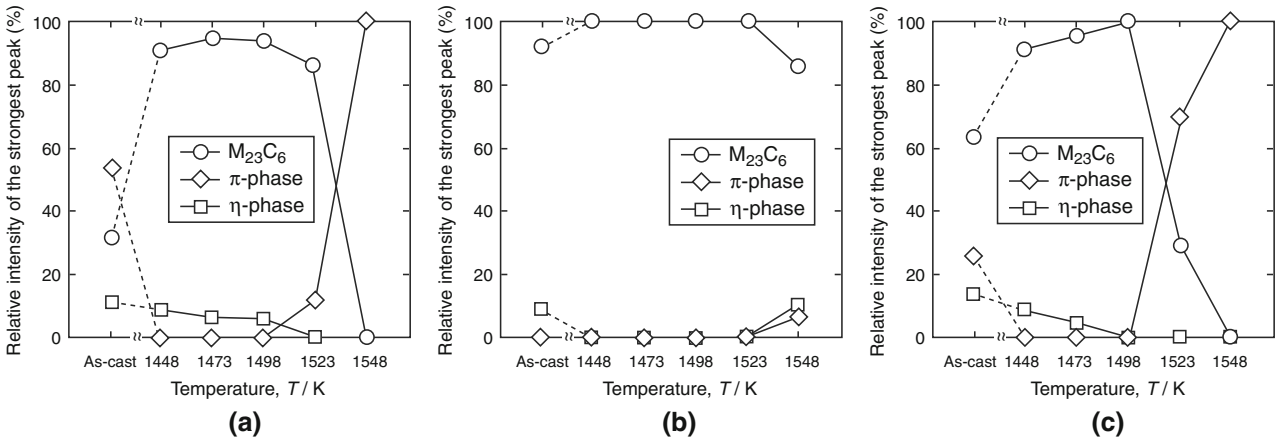

Fig. 11—Relative intensities of the strongest peaks in the XRD patterns for each precipitate in the (*a*) 1Si, (*b*) 1Mn, and (*c*) 1Si1Mn alloys after heat treatment at various temperatures for 0 ks.

V. CONCLUSIONS

The effects of the addition of 1 mass pct Si and/or 1 mass pct Mn in Co-28Cr-6Mo-0.25C alloys on precipitates before and after heat treatment over the temperature range of 1448 K to 1548 K (1175 °C to 1275 °C) were investigated. The following results were obtained.

1. The microstructure observed in the as-cast alloys was affected by the addition of Si and/or Mn. The precipitates in the as-cast 1Si and 1Si1Mn alloys were $M_{23}C_6$-type carbide, η phase (M_6C-$M_{12}C$-type carbide), and π phase (M_2T_3X-type carbide with a β-Mn structure); $M_{23}C_6$-type carbide and η phase were observed in the as-cast 1Mn alloy.
2. Complete precipitate dissolution was achieved in all the alloys. The addition of Si increased the holding time for complete precipitate dissolution, whereas the precipitates in the 1Mn alloy dissolved in a short holding time.
3. An $M_{23}C_6$-type carbide, an η phase, and a π phase were observed as precipitates during the solution treatment. The π phase was observed in the 1Si and 1Si1Mn alloys heat treated at 1523 K and 1548 K (1250 °C and 1275 °C) and in the 1Mn alloy heat treated at 1548 K (1275 °C), while it was the primary precipitate in the 1Si and 1Si1Mn alloys heat treated at 1548 K (1275 °C).
4. The morphologies of the precipitates in the alloys depended on the heat-treatment temperature and alloy composition. The blocky dense $M_{23}C_6$-type carbide was observed in all the alloys heat treated over the lower temperature range of 1448 K to 1498 K (1175 °C to 1225 °C). At higher temperatures, such as 1548 K (1275 °C), two types of starlike precipitates—dense and stripe patterned—were observed. The starlike-dense precipitate was the π phase, while the starlike precipitate with stripe patterns was identified as the $M_{23}C_6$-type carbide and metallic fcc γ phase.
5. The π-phase formation and starlike morphology appear to be closely related to the partial melting in the alloys caused by nonuniformities in the as-cast alloys. The addition of Si and Mn decreases the partial melting temperature to promote the π-phase formation and starlike morphology.

ACKNOWLEDGMENTS

The authors thank Yoneda Advanced Casting Co., Ltd. for supplying the Co-Cr-Mo alloy ingots used in this study, Mr. K. Suda for his FE EMPA measurements, and Dr. K. Kobayashi for his TEM works.

REFERENCES

1. ASTM F75–07, *Annual Book of ASTM Standards*, ASTM International, West Conshohocken, PA, 2008, vol. 13.01, pp. 64–66.

2. L.E. Ramírez, M. Castro, M. Méndez, J. Lacaze, M. Herrera, and G. Lesoult: *Scripta Mater*., 2002, vol. 47, pp. 811–16.
3. M. Niinomi, T. Hanawa, and T. Narushima: *JOM*, 2005, vol. 57 (4), pp. 18–24.
4. S.H. Lee, N. Nomura, and A. Chiba: *Mater. Trans*., 2008, vol. 49, pp. 260–64.
5. M. Niinomi: *Metall. Mater. Trans. A*, 2002, vol. 33A, pp. 477–86.
6. J.W. Weeton and R.A. Signorelli: *Trans. Am. Soc. Met*., 1955, vol. 47, pp. 815–45.
7. K. Asgar and F.A. Peyton: *J. Dent. Res*., 1961, vol. 40, pp. 73–86.
8. A.J.T. Clemow and B.L. Daniell: *J. Biomed. Mater. Res*., 1979, vol. 13, pp. 265–79.
9. T. Kilner, R.M. Pilliar, G.C. Weatherly, and C. Allibert: *J. Biomed. Mater. Res*., 1982, vol. 16, pp. 63–79.
10. S. Mineta, S. Namba, T. Yoneda, K. Ueda, and T. Narushima: *Metall. Mater. Trans. A*, 2010, vol. 41A, pp. 2129–38.
11. D.S. Janisch, M. Garel, A. Eder, W. Lengauer, K. Dreyer, and H. van den Berg: *Int. J. Refract. Met. Hard Mater*., 2008, vol. 26, pp. 179–89.
12. A.C. Fraker and H.H. Stadelmaier: *Trans. TMS- AIME*, 1969, vol. 245, pp. 847–50.
13. J.M. Guilemany, J.M. de Paco, J. Nutting, and J.R. Miguel: *Metall. Mater. Trans. A*, 1999, vol. 30A, pp. 1913–21.
14. J. Jeciejewicz: *J. Less-Common Met*., 1964, vol. 7, pp. 318–20.
15. H.S. Dobbs and J.L.M. Robertson: *J. Mater. Sci*., 1983, vol. 18, pp. 391–401.
16. M. Caudillo, M. Herrera-Trejo, M.R. Castro, E. Ramírez, C.R. González, and J.I. Juárez: *J. Biomed. Mater. Res*., 2002, vol. 59, pp. 378–85.
17. M. Herrera, A. Espinoza, J. Méndez, M. Castro, J. López, and J. Rendón: *J. Mater. Sci.: Mater. Med*., 2005, vol. 16, pp. 607–11.
18. H. Mancha, E. Carranza, J.I. Escalante, G. Mendoza, M. Méndez, F. Cepeda, and E. Valdés: *Metall. Mater. Trans. A*, 2001, vol. 32A, pp. 979–84.
19. Montero-Ocampo, M. Talavera, and H. Lopez: *Metall. Mater. Trans. A*, 1999, vol. 30A, pp. 611–20.
20. R.N.J. Taylor and R.B. Waterhouse: *J. Mater. Sci*., 1983, vol. 18, pp. 3265–80.
21. S.H. Lee, N. Nomura, and A. Chiba: *Mater. Trans*., 2007, vol. 48, pp. 2207–11.
22. Z. de la Garza, M. Herrera-Trejo, M. Castro R., E. Ramírez V., M. Mendez N., and J. Mendez N.: *J. Mater. Eng. Perform*., 2001, vol. 10, pp. 153–56.
23. JCPDS card no. 26-0428.
24. M. Kikuchi, S. Wakita, and R. Tanaka: *Trans. ISIJ*, 1973, vol. 13, pp. 226–28.
25. S. Wakita, M. Kikuchi, and R. Tanaka: *Tetsu-to-Hagané*, 1975, vol. 61, pp. 2418–32.
26. M. Kikuchi, T. Sekita, S. Wakita, and R. Tanaka: *Tetsu-to-Hagané*, 1981, vol. 67, pp. 1981–89.
27. B.C. De Cooman: *Curr. Opin. Solid State Mater. Sci*., 2004, vol. 8, pp. 285–303.